

2013

# Clay Mineralogy of the MH-2 Core, Snake River Plain, Idaho

Joe Wheeler

Follow this and additional works at: [http://digitalwindow.vassar.edu/senior\\_capstone](http://digitalwindow.vassar.edu/senior_capstone)

---

## Recommended Citation

Wheeler, Joe, "Clay Mineralogy of the MH-2 Core, Snake River Plain, Idaho" (2013). *Senior Capstone Projects*. 239.  
[http://digitalwindow.vassar.edu/senior\\_capstone/239](http://digitalwindow.vassar.edu/senior_capstone/239)

This Open Access is brought to you for free and open access by Digital Window @ Vassar. It has been accepted for inclusion in Senior Capstone Projects by an authorized administrator of Digital Window @ Vassar. For more information, please contact [library\\_thesis@vassar.edu](mailto:library_thesis@vassar.edu).

# **Clay Mineralogy of the MH-2 Core, Snake River Plain, Idaho**

Joe Wheeler

May 2013

*Department of Earth Science and Geography, Vassar College,  
Poughkeepsie, NY*

Senior Thesis

Submitted in partial fulfillment of the requirements for the Bachelor of Arts degree  
in Earth Science

---

Adviser, Jeff Walker

## **Abstract**

The MH-2B hole was one of three holes completed as a part of HOTSPOT: The Continental Scientific Drilling Project. MH-2B was drilled to a depth of 1821m on the Mountain Home Air Force Base southeast of Boise, Idaho to evaluate the potential for development for geothermal energy on the base. Water under artesian pressure was encountered at a depth of 1745 m. We analyzed pieces of the core to study clay mineralization with depth. We took 22 samples from the bottom half of the core, focusing on around 1790m, where preliminary analysis indicated the presence of corrensite (R1 ordered smectite/chlorite). X-ray diffraction (XRD) of these powders showed a transition from smectite at 762m to corrensite at 1790m and back to smectite at 1807m. More detailed XRD analysis with ethylene-glycol solvated samples confirmed the findings of the powder samples (namely a transition from smectite -> corrensite -> smectite). We modeled smectite and corrensite crystallinity with depth and found an increase in the defect free distance of both minerals. Samples around 1790m showed the presence of smectite, corrensite, and possibly chlorite (or serpentine). We interpret this result to support a discontinuous (stepwise) model for the smectite-chlorite transition. The presence of artesian fluid in this zone is evidence for the importance of high fluid/rock ratios in the smectite-chlorite transition, and the association of high fluid/rock ratios with a discontinuous transition model.

## **Introduction**

### *Geologic Setting*

The Snake River volcanic province (SRP) in central Idaho was created when North America moved over a mantle hotspot (which is now beneath Yellowstone) in the late Cenozoic (Aly et al. 2009). The plain spans roughly 500 km through southern Idaho (Figure 1) and is covered by basalt and interbedded continental sediments (Breckenridge et al. 2012). The region has some of the highest heat flow in North America and is one of the United States' most underdeveloped geothermal resources (Shervais et al. 2011). Thermal gradients are elevated throughout the region. They are highest along the margins of the Snake River plain and lowest along the axis, where the Snake River aquifer suppresses temperatures (Shervais et al.

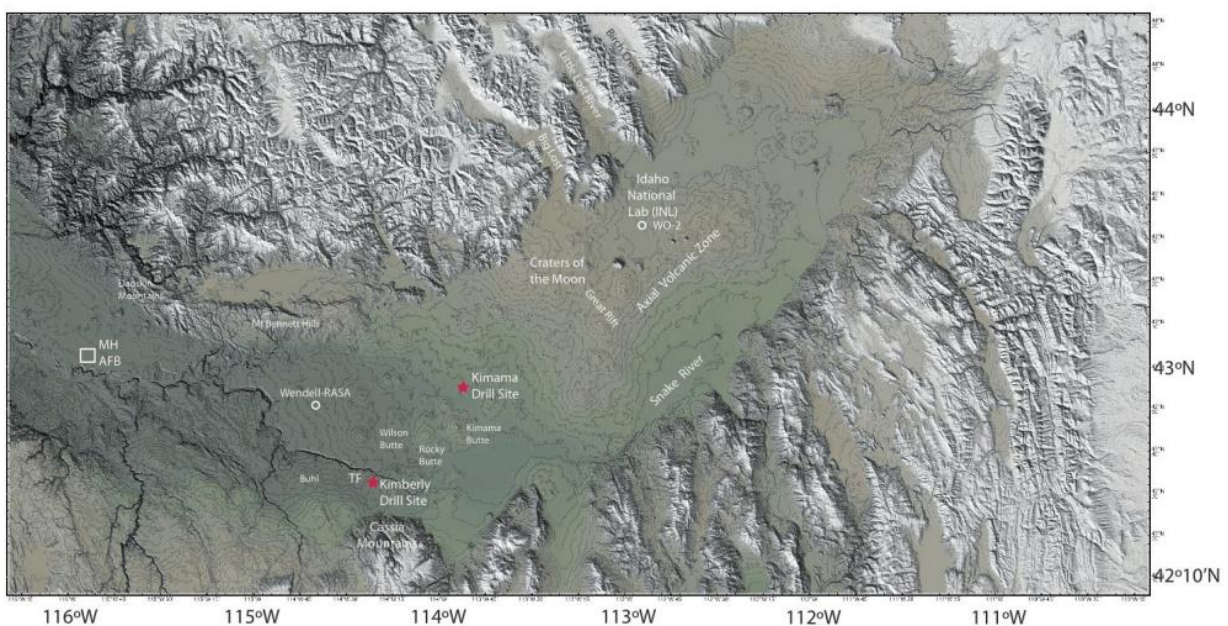


**Figure 1 Shaded relief-topographic map of Snake River Plain derived from NASA 10m DEM data and contoured at 30m intervals. Red stars = new drill sites of this project; open circles = legacy drill sites. (Shervais et al. 2011).**

2011).

Since September 2010, Project Hotspot, an international group investigating the region, has studied the thermal system and its relationship to the path of the

active Yellowstone hotspot. One of

the project's goals is to

understand the compositional

relationship between the

Yellowstone Plateau – which is

composed of rhyolite and

ignimbrites – and the Snake River

Plain – which is underlain by

basalt and plume-derived rhyolite.

The project has drilled three

intermediate depth wells in the

region as part of its process.

The third and most recent

well, MH-2, was drilled primarily

to examine the geothermal

potential of the Mountain Home

Air Force Base (MHAFB).

Geothermal energy for the region

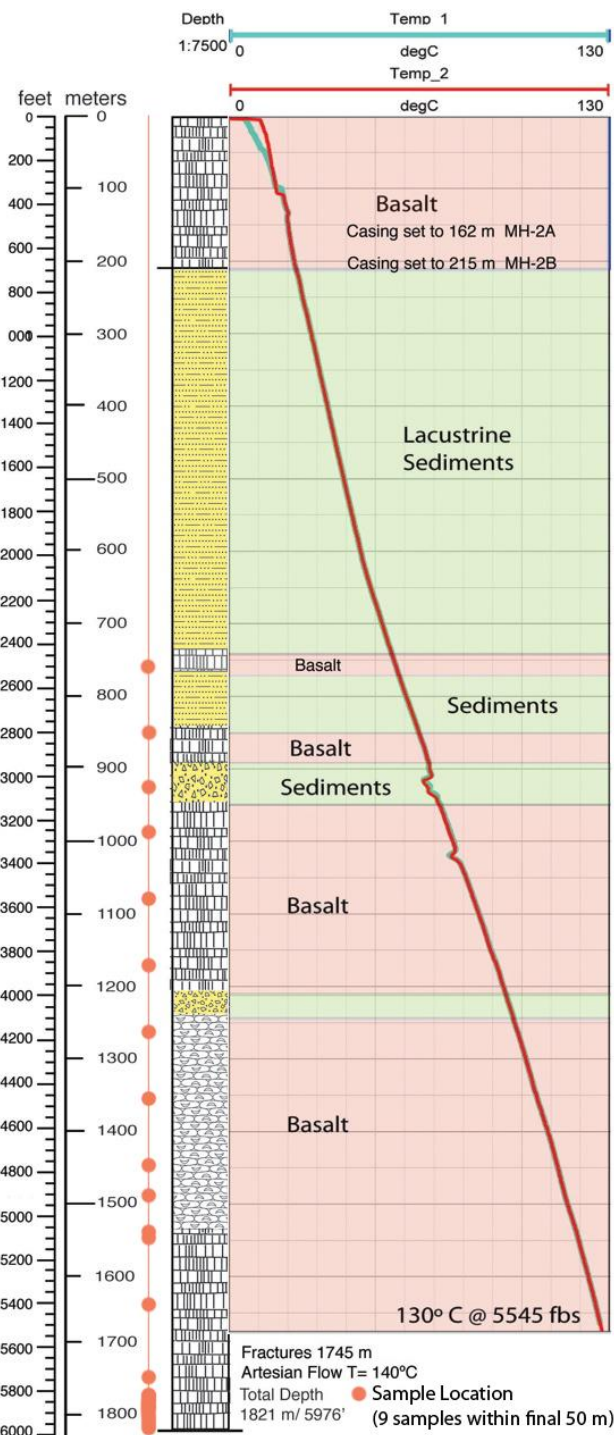


**Figure 2** Lithologic and temperature logs of the MH-2 core. Our sample locations are represented by orange dots. There are 9 samples within the final 50m of the core.

has at present been limited to only one commercial plant: the Raft River Geothermal Plant approximately 150 miles SE of the Mountain Home site. The Snake River Plain also currently has numerous small-scale direct-use applications including space heating and aquaculture (Shervais et al. 2011). Despite this underutilization, the large scale power generation potential is high. The U.S. Air Force hopes to use geothermal power as a safe and secure energy source for the base. MH-1, the first exploratory well was drilled on the base in 1986 and then plugged. Drilling for the current well, MH-2, began in July 2011 and was finished in January 2012. When operations were completed the well went to a total depth of 1821m (Breckenridge et al. 2012). The general lithology of the well (starting at the surface) is as follows:  $\approx$ 210 m of basalt,  $\approx$ 610 m of lake sediments, and  $\approx$ 915 m of increasingly altered basalt (Figure 2). Temperatures at 1700m were measured at 130°C; at the bottom of the well (where temperatures were not measured) they were estimated to be roughly 140°C (Breckenridge et al. 2012). Drillers encountered a fracture system with water under artesian pressure at a depth of 1745 m. The water was analyzed and shown to be sulfate-rich and Cl-poor with low pH ( $\approx$ 5.6-5.7) (Breckenridge et al. 2012). These water characteristics suggest steam-heated volcanic waters equilibrated with altered basalt (Breckenridge et al. 2012). Current studies, including this paper, hope to aid the base in characterization of porosity and permeability of the rocks and to contribute to a more thorough understanding of the minerals formed by hydrothermal alteration. It remains unknown whether permeability, volume of water, and available heat are sufficient for electrical generation (Breckenridge et al. 2012).

### Clay Mineralogy

Clay minerals are layered aluminum silicates by definition smaller than 2  $\mu\text{m}$  equivalent spherical diameter (e.s.d.). They are the most abundant minerals on the surface of the earth (Moore and Reynolds, 1). The structural layers are made of two different sheets, one with oxygen in tetrahedral coordination around Si or Al, the other with O and OH in octahedral coordination around  $\text{Mg}^{2+}$  and  $\text{Fe}^{2+}$ , or  $\text{Al}^{3+}$ . The tetrahedra form hexagonal sheets designated by "T". Octahedral sheets, designated

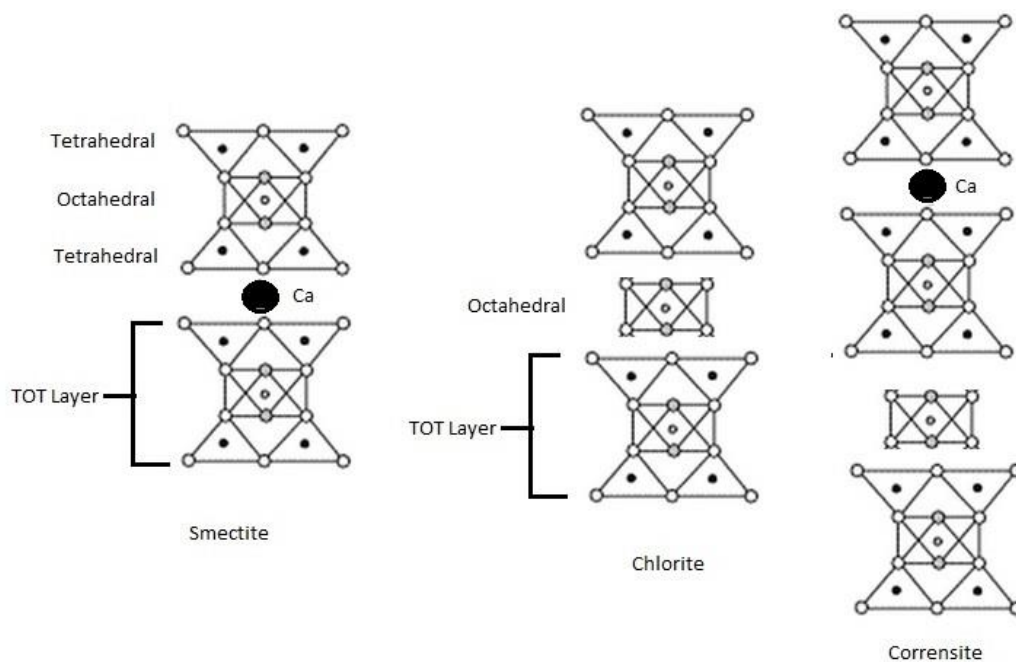


**Figure 3** Diagrams for smectite, chlorite, and corrensite. All three clays are made up of TOT layer. The difference lies in the nature of the interlayer. (Figure modified from Nelson 2011)

by "O", may be either dioctahedral or trioctahedral depending on the number of divalent or trivalent cations necessary to achieve electrical neutrality: three 2+ cations (trioctahedral) or two 3+ cations (dioctahedral). Clay mineral structures

involve stacks of either 2 sheets (TO) or 3 sheets (TOT) to create the basic layer (Figure 3). These sheets are held together by relatively weak Van der Waals bonds, interlayer cations (micas), hydrated interlayer cations (smectite), or other octahedral layers (chlorite).

Preliminary research has indicated the presence of three clay minerals within the MH-2 core: smectite, chlorite, and corrensite. Smectites are a group of dioctahedral and trioctahedral clay minerals that have expandable crystallographic structures (Moore and Reynolds, 136). Due to a small interlayer charge ( $\sim 0.33$  /layer), water or an organic compound, such as ethylene glycol, can enter and expand the interlayer of a crystal. In volcanic and volcani-clastic systems, the mineral has been interpreted to form from the alteration of silica rich volcanic glass (Moore and Reynolds, 138). When expanded with ethylene glycol, the spacing between two smectite layers ( $d_{001}$ ) is a uniform 16.9 Å.

Chlorite appears to form from metamorphosed smectite. It is also arranged in trioctahedral TOT layers, but the interlayer is made up of another O sheet. The  $d_{001}$  value for chlorite is 14.2 Å. Corrensite is a mixed-layer clay mineral composed of an R1 ordered (one-to-one) mixture of smectite and chlorite. The  $d_{001}$  for glycolated corrensite is about 31 Å (16.9 Å for smectite + 14.2 Å for chlorite). These three minerals all have TOT similar layers and differ mostly by the nature of their interlayer. Because the TOT layer is basically the same for all three, only an interlayer change is needed to transition from one to another.

## X-ray Diffraction

X-ray diffraction (XRD) analysis consists of measuring the reflection (diffraction) of an X-ray beam off the crystal structure of a mineral. As emitted waves reflect off different atomic planes of the crystal they undergo either

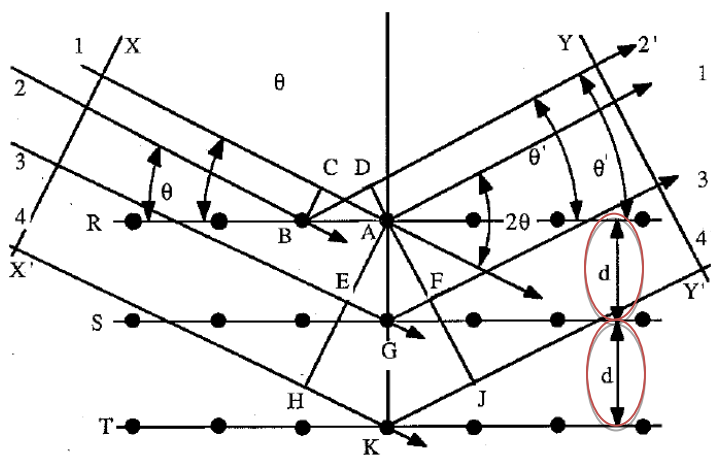


Figure 4 Diffraction between rows of atoms. The  $d$  value is the spacing between diffracting domains. (Moore and Reynolds 68).

constructive or destructive interference. In the case of constructive interference – when wavelengths are in phase – X-rays are reflected back from the mineral and measured by a detector as individual peaks. By

measuring the angle at which constructive interference occurs and the wavelength of the X-ray, the spacing between reflecting planes (the  $d$  value) can be calculated (Figure 4). The spacing of these planes correlates to a distinct mineral structure. The positions and relative intensities X-ray peaks are used to identify an unknown mineral.

Because of their structure, clay minerals behave uniquely under XRD. Clay minerals are made up of layers that extend in the horizontal plane but have a limited number of layers stacked on top of each other, creating relatively thin diffracting

domains and producing broader peaks than those of more crystalline minerals. The width of individual peaks can be used to estimate the average number of unit cells stacked together without a defect. In addition, because clays are structured in layers, constructive interference can occur between 2 layers, and also between two or more layers (these are known as basal reflections or the  $00l$  series). Diffraction between multiple layers of parallel sheets creates rationally spaced peaks useful in clay identification. Because smectite, chlorite, and corrensite are TOT clays, stacking differences and the nature of interlayering are what differentiate the three minerals. XRD displays these differences and so makes it possible to distinguish between the three clay types.

### *The Smectite-Chlorite Transition*

The smectite to chlorite transition is a poorly understood facet of low-grade metamorphism. The details of this conversion, particularly the nature of intermediate stages are the subject of debate in scientific literature. It is uncertain whether the transition is continuous, with even growth of randomly interstratified (R0) chlorite-smectite (C-S), or whether the transition is discontinuous (stepwise), with no intermediates between smectite, corrensite, and chlorite. A continuous conversion includes R0 C-S, while a discontinuous process has only regularly ordered C-S also known as corrensite.

Schiffman and Fridleifsson (1991) looked at clays within a basaltic core from Iceland. They found smectite at temperatures below 180°C, randomly interstratified chlorite and smectite between 200°C and 240°C, regularly (R1) and randomly interstratified chlorite-smectite between 245°C and 265°C, and discrete chlorite above 270°C. Bettison-Varga and Mackinnon (1997) looked at phyllosilicates in a hydrothermally altered basalt from California with transmission electron microscopy (TEM). They found large crystals of randomly interstratified chlorite-smectite and suggest that the process is continuous with dissolution and re-precipitation as key mechanisms in formation. Murakami et al. (1999) on the other hand, found with TEM that the transition occurs stepwise from smectite to corrensite and from corrensite to chlorite. They also found dissolution and precipitation to be the dominant mechanisms. This discontinuous model, although newer, is supported by results of laboratory experiments (Roberson et al. 1999). Robinson and Zamora (1999), found no corrensite in their study of exploratory wells from the Chipilapa geothermal system in El Salvador, but they too determined the smectite to chlorite transition to be stepwise, with no randomly interstratified chlorite-smectite.

The difference between the continuous and the discontinuous reactions might be controlled by fluid/rock ratios. Areas with high permeability and high fluid/rock ratios have been shown to be associated with the discontinuous model while continuous sequences are associated with low ratios (Dekayir et al. 2005, Schmidt and Robinson 1997, Shau and Pecor 1992). The presence of discrete

minerals, with no random mixed-layer C-S has also been shown to correspond to equilibrated systems (Shau and Pecor 1992). Threshold temperatures for reactions of either model are approximately 150°C (Schmidt and Robinson 1997).

This study used X-ray Diffraction techniques to look in detail at the clay mineralogy of the MH-2 core, and to investigate the nature and behavior of the clay minerals with changes in depth. The crystallization changes within individual minerals (smectite and corrensite) with depth are examined as well as the nature of the smectite-chlorite transition. We hope to contribute to the current debate regarding the nature of the transition from smectite to chlorite.

## Methods

Twenty-three samples from between 750m and 1820m (see Figure 2) depth were collected from the MH-2 core. Ten samples were taken from 1750m to 1820m because of the presence of geothermal or hydrothermal fluid, and because preliminary results indicated the presence of corrensite. The rest of the core was evenly

sampled approximately every 100m. We focused on and sampled only basaltic sections of the core.



With depth **Figure 5 The basaltic section of the core at 1763m, the heart of the section most intensely studied. Photo credit: Project Hotspot**

the core changes from sandy tan sediments to greenish grey basalts. It is mostly fine-grained but at deeper intervals it shows some visible crystals and alterations (Breckenridge et al. 2012). Figure 5 shows an example of the core in the corrensite bearing range (1763m).

All 23 samples were crushed and ground in a Cole Parmer model 4301 analytic mill and then were sieved to a <250- $\mu\text{m}$  grain size using an ASTM sieve. Well slides were filled with these random powders for initial XRD analysis.

X-ray diffraction analyses were performed on these samples at Vassar College using a Bruker D2 diffractometer at 30kV and 10mA with a  $0.6^\circ$  incident beam slit size. Samples were routinely run with an 0.1 step size and a count time ranging from 0.4 to 1.0 sec/step from  $2^\circ$  to  $35^\circ 2\theta$ .

XRD patterns were analyzed with Bruker DIFFRAC.EVA V2.1. This software was used to overlay different patterns and to calculate XRD characteristics (including position, intensity, and full width at half maximum (FWHM) of peaks).

From the 23 random powder mounts, we chose ten representative samples for more detailed study. Oriented mounts of the less than  $2\mu\text{m}$  e.s.d. clay fractions were prepared by ultrasonic treatment of the powder suspended in water with a Branson Sonifier 250 for approximately one minute. The resulting suspension was centrifuged in a Beckman Model TJ-6 for three minutes at 750 rpm to settle out  $>2\mu\text{m}$  e.s.d. fractions. This suspension was vacuum filtered through a  $0.45\text{-}\mu\text{m}$  milipore filter. We then attempted to transfer the clay to a slide by drying the filter on a 3.5 cm glass slide. If this proved unsuccessful we re-sonified the clay and spread it evenly on a glass slide by pipetting.

Air-dried samples were analyzed with the same parameters as above. After this, each sample was exposed to ethylene glycol vapor at  $60^\circ\text{C}$  for at least 24 hours. The glycolated samples were analyzed with the same parameters.

The original glycolated clays showed patterns with peak values that were slightly off. The corrensite peak for the 1791m sample, for example, had a d value of  $\approx 29.5 \text{ \AA}$  ( $\approx 3^\circ 2\theta$ ) whereas the corrensite peak is normally at  $\approx 31 \text{ \AA}$ . This was solved by calcium saturating the samples. Figure 6 shows the difference between a saturated and unsaturated sample. Because the calcium-saturated samples have correct peak placements, all samples were Ca-saturated.

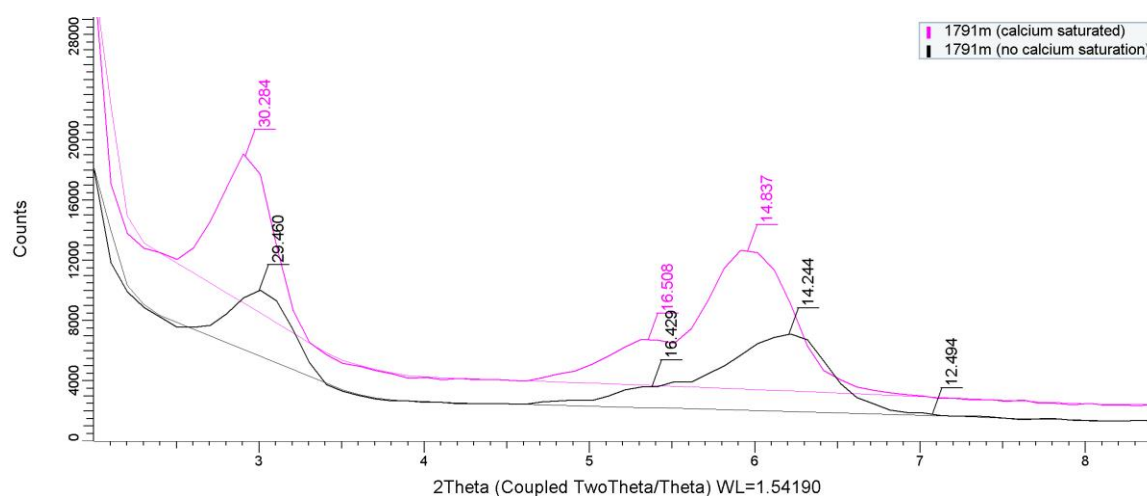


**Figure 6** The effect of calcium saturation on peak placement. The saturated samples had peak locations in expected locations while unsaturated samples were at a higher angle than expected

Calcium saturation was done by exposing the re-sonified  $<2\text{-}\mu\text{m}$  to  $\approx 50\text{mL}$   $0.1\text{M}$  calcium chloride solution for  $\approx$ two minutes. The samples were rinsed with  $\approx 150\text{mL}$  of water and spread evenly on a glass slide with pipette. The calcium-saturated samples were analyzed using XRD (same as above) as both air-dried and glycolated samples.

Modeling of XRD patterns was done with the NEWMOD modeling software (versions one and two). This software was used to estimate relative compositions of clay types, the nature of interstratification (R0 or R1), and to estimate mean defect free distance of crystals. We followed an example set by Beaufort and Meunier

(1994) and used 0.38 as a value for Fe atoms because we were unable to measure this value for ourselves.

## Results

### *Randomly Oriented Powder Mounts*

Figure 7a shows four representative diffraction patterns for the random powder mounts, which were used to determine which samples should be investigated in more detail. The results show a trend from smectite to corrensite (at about 1790m) and back to smectite. The numerous sharp peaks are from plagioclase feldspars and zeolites such as laumontite. Figure 7b shows 4 representative samples plotted in depth order on the same graph. Patterns around 1750m are clearly distinct from the other portions of the core.

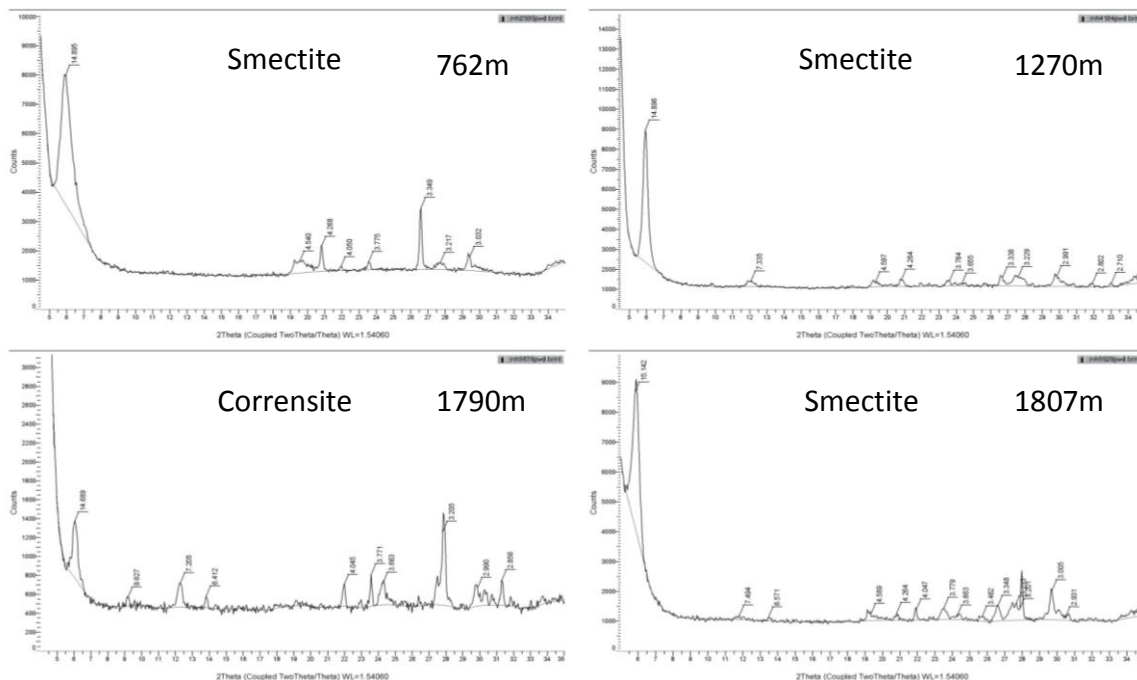


**Figure 7a Four Representative diffraction patterns for random powder mounts. 762m, 1270m, and 1807, all indicate smectite. 1790m is clearly different and the pattern suggests corrensite.**

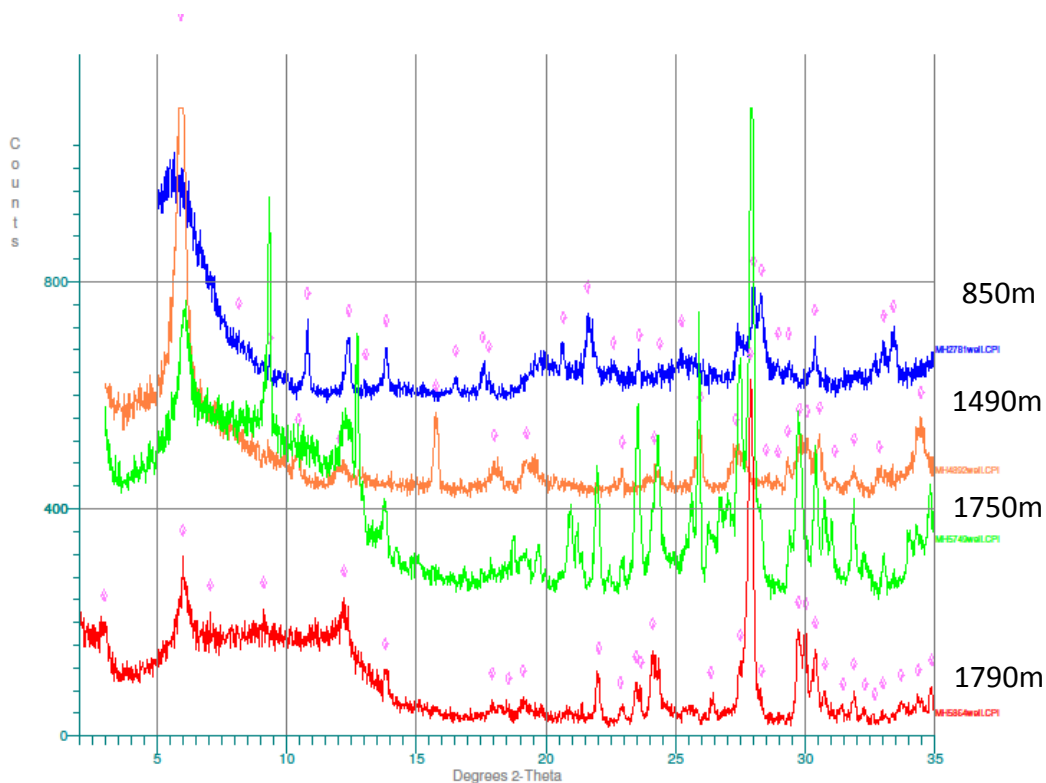


Figure 7b Four powder patterns arranged in order of depth. The third sample has a unique peak at  $\approx 10^\circ$ . This data helped us pick samples for more detailed study.

### *Glycolated Filter Peels*

Of the eight calcium-saturated and glycolated samples, three (762m, 1555m, and 1807m) were pure smectite. Figure 8 shows these samples zoomed in on the  $d_{001}$  peak ( $\approx 17\text{\AA}$ ). It is clear that the peak sharpness increases as depth increases. Modeled changes of Full Width at Half Maximum (FWHM or  $\beta$ ) show that the mean defect free distance ( $\delta$ ) of the smectite increases with depth (Table 1). The general effects of a changing  $\delta$  value (as modeled in NEWMOD) are demonstrated in Figure

9.

Smectite			
Depth (m)	Measured FWHM ( $\beta$ )	Modeled $\delta$	Modeled FWHM ( $\beta$ )
762	1.26	1.5	1.26
1555	0.281	7	0.28
1807	0.241	10	0.24

Table 1 Modeled and measured FWHM ( $\beta$ ) and defect-free distance ( $\delta$ ). With depth the measured value of smectite  $\beta$  increases. The model of this increase has a corresponding increase for  $\delta$  values.

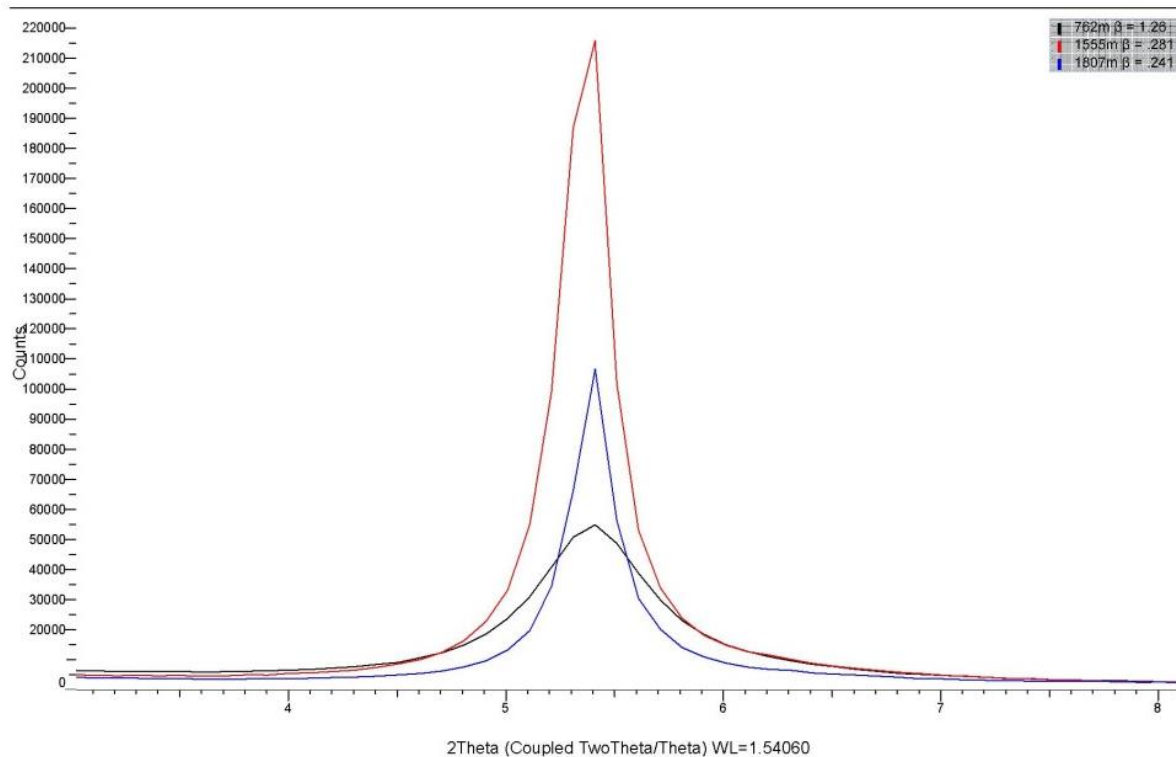


Figure 8 Changing width of the (001) smectite peak. With depth the peaks get less broad

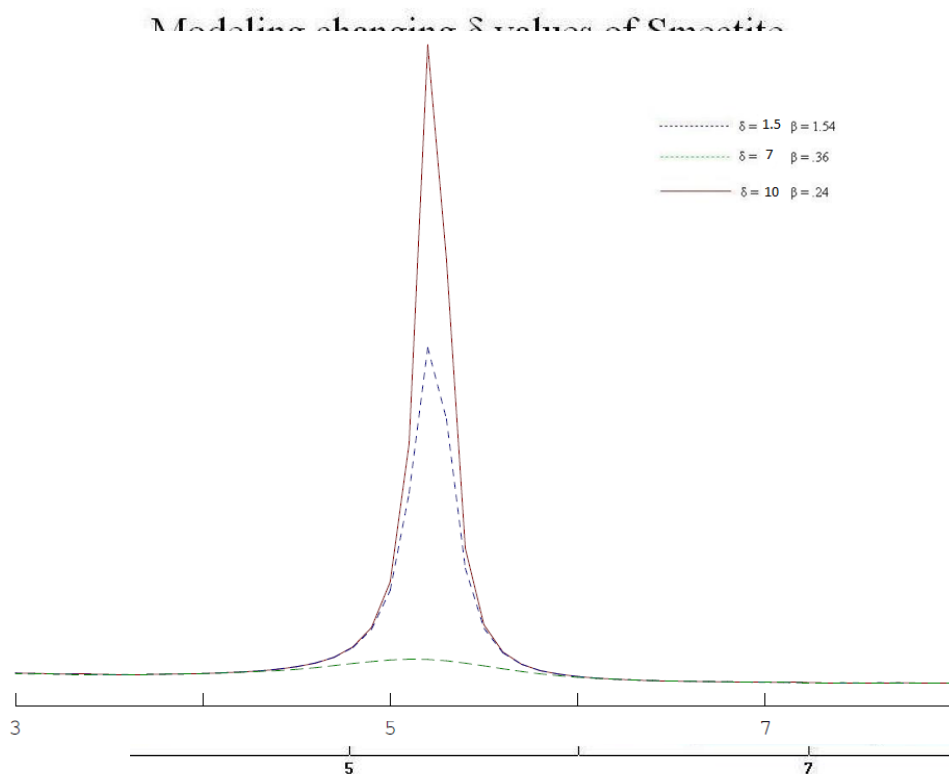
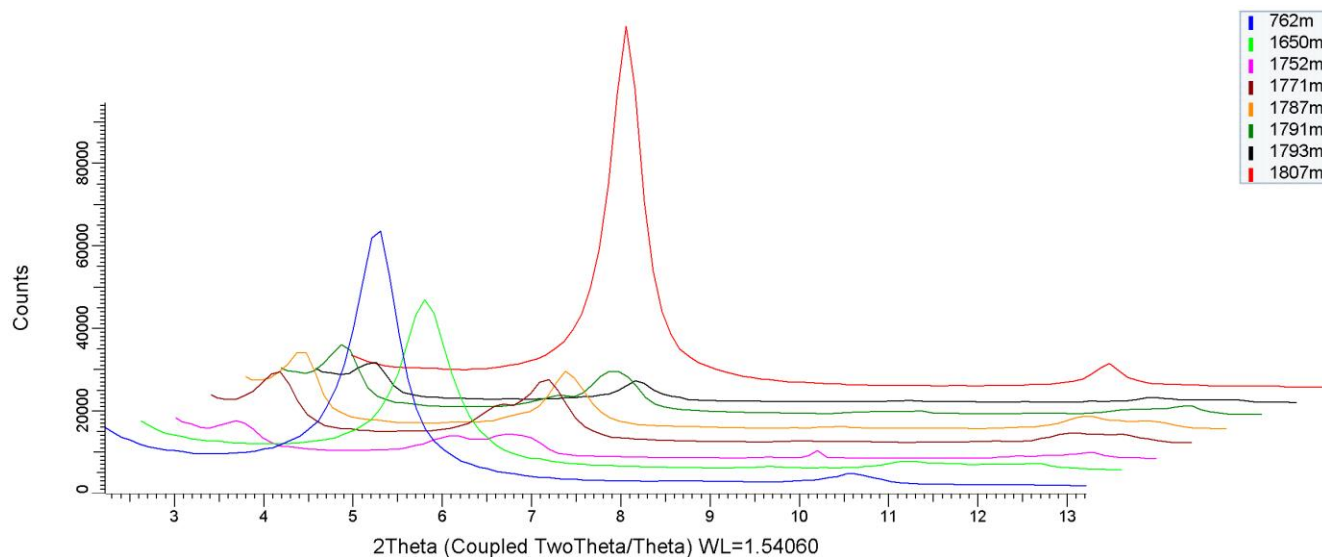


Figure 9 NEWMOD modeling patterns for increased defect-free distance ( $\delta$ ). With increases in  $\delta$  peaks get sharper and taller, similar to the measured patterns in figure 8.

Diffraction patterns for all eight samples are shown in Figure 10. Clay minerals in the core transition from pure smectite to a corrensite-bearing zone at  $\approx 1752\text{m}$  and then back to smectite at  $\approx 1807\text{m}$ . This matches the powder mount results but also shows the corrensite zone to be more complicated than indicated by



**Figure 10** The diffraction patterns for all 8 closely studied samples. The transition from smectite to a corrensite-bearing zone to another smectite zone is clearly seen.

powder analysis. XRD results of these samples are summarized in Tables 2a&b.

Samples from 1787m and 1793m have both corrensite and chlorite peaks. Samples from 1752m, 1771m, and 1791m appear to have smectite ( $d_{001}$ ,  $d_{005}$ , and  $d_{006}$  peaks), corrensite ( $d_{001}$ ,  $d_{002}$ ,  $d_{003}$ ,  $d_{004}$ , and  $d_{005}$  peaks), and chlorite (the  $d_{002}$  peak). The pattern for 1752m (figure 11) shows representative mineral peaks. The chlorite peak could be serpentine (which also generates a peak at  $7.1\text{\AA}$ ) but the asymmetry on the high-angle side of the corrensite  $d_{002}$  peaks (figure 11) suggests that a weak chlorite  $d_{001}$  peak may be combined with the corrensite peak.

We calculated the coefficient of variation (CV) for the  $d_{001}$  peak series' for both smectite and corrensite (table 2b). There were not enough measurable peaks

to draw strong conclusions from this data, but corrensite peaks generally had a much higher CV value than smectite peaks. The fact that corrensite peaks - which occur exclusively in the altered zone - are less rational than smectite could be evidence for the presence of random interstratification of chlorite-smectite as well

Depth (m)	Distinct Peaks (d value):									
	c d001	s d001	c d002	c d003	s d002	c d004	ch d002	c d005	s d005	s d006
762		16.926			8.409				3.317	
1650		16.32		9.591	8.116		7.314			
1752	30.644	16.561	14.794	9.385		7.467	7.118	6.363	3.31	2.707
1771	29.404	15.912	14.462	9.412		7.4	7.122	6.324		2.698
1787	31.333		15.152	9.937		7.588	7.185	6.369		2.705
1791	30.5	16.414	14.824	9.449		7.475	7.161	6.363		2.706
1793	31.371		15.174			7.601	7.106	6.358		2.704
1807		16.683			8.255				3.303	

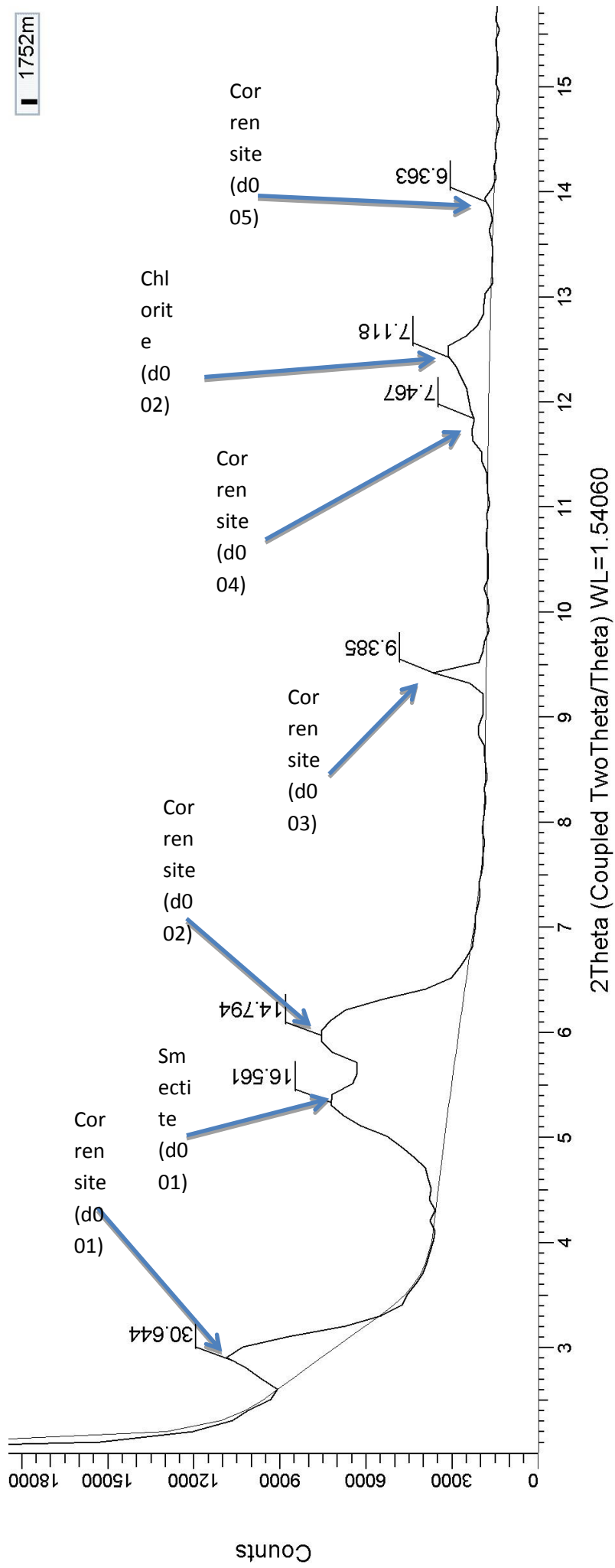
**Table 2a The measurable peaks for all 8 closely studied samples. Peak locations were calculated with DIFFRAC.EVA V2.1  
c = corrensite s = smectite ch = chlorite**

Depth (m)	Smectite?	CV of peaks	Corrensite?	CV of peaks	Possible Chlorite peak?
762	Yes	1.0388	-	-	-
1650	Yes	0.3823	Yes	Only 1 peak	Yes
1752	Yes	0.047	Yes	4.5	Yes
1771	Yes	1.215	Yes	4.288	Yes
1787	-	-	Yes	2.478	Yes
1791	Yes	0.771	Yes	4.211	Yes
1793	-	-	Yes	2.313	Yes
1807	Yes	0.594	-	-	-

**Table 2b Possible clay minerals present in each sample. The rationality (coefficient of variation) was calculated for smectite and corrensite peaks.**

as corrensite. The presence of randomly interstratified chlorite-smectite would create high variation among the corrensite peaks. Further research should clarify the rationality of peaks to explore this possibility

1752m



## **Discussion and Conclusions**

### *Characterization of Core*

XRD analysis of the core shows smectite to be the dominant clay mineral throughout the core. With increases in depth and temperature smectites appear to become more crystalline. The measured FWHM for the  $d_{001}$  peak decreases from 1.26 at 762m to .281 at 1555m to .241 at 1807m. Modeled defect-free distance increases from 1.5 to 7 to 10 in the same three samples. Corrensite crystallinity also seems to increase with depth. The measured FWHM for the  $d_{001}$  peak decreases from 0.633 at 1650m to .497 at 1787m, to .426 at 1807m. The corresponding modeled defect-free distance increases from 3.2 to 4 to 5.4 respectively. The increasing defect free distance for both crystals suggests, as we might expect, that the clays become more perfectly formed as depth and temperature increases. Smectite, dominant at both the top and bottom of the basalt zone of the core, correlates with increases in pressure and temperature, suggesting that these are the most important variables.

Because of its confinement to a relatively thin zone, other variables must have been at work in the sections containing corrensite. Our data agree with the work of others (Dekayir et al. 2005, Schmidt and Robinson 1997, Shau and Pecor 1992) in that the high fluid/rock ratio beginning around 1745m seems to have made metamorphism possible. Fluid seems to be the variable that explains such rapid compositional changes over such limited depth and temperature changes.

The results of XRD analysis from 1752m – 1793 are evidence for the simultaneous and discrete presence of smectite, corrensite, and possibly chlorite. Samples from this range have peaks indicative of all three minerals. The strongest evidence for corrensite is the superlattice peak at  $\approx 31 \text{ \AA}$ , which is present in all samples of this range. Three of the five (1752, 1771, 1791) also have two peaks at around  $6^\circ 2\theta$  that are interpreted to correspond to the smectite  $d_{001}$  and corrensite  $d_{002}$  peaks. While the samples at 1787m and 1793m have only one peak in this region, the peak for both is located at around  $15^\circ 2\theta$ , or directly between the positions of smectite  $d_{001}$  and corrensite  $d_{002}$  peaks. It is possible that these samples have both peaks, but that they were not resolved by our scans. The co-existence of all three clay minerals – but particularly of the smectite and corrensite peaks (see figure 11) – in this range is strong XRD evidence for the existence of all three minerals as discrete phases. We found no conclusive evidence for randomly interstratified chlorite-smectite. This data fits well with other recent characterizations of smectite – chlorite transitions. The correlation between high fluid/rock ratios and a discontinuous transition as described by Shau and Pecor (1992) is reflected in our data. There is also evidence for the other side of this model – that low fluid/rock ratios are associated with a continuous sequence – in the sample from 1650m. This sample, which is above the zone with water, has the smectite ( $d_{001}$   $d_{002}$ ) and the chlorite ( $d_{002}$ ) peaks, but no corrensite superlattice peak, and only a very weak corrensite  $d_{003}$  peak. This could be evidence for randomly interstratified C-S in this sample.

The temperature of the artesian well water in the alteration zone (140°C) fits well with the findings of Schmidt and Robinson (1997), who found that corrensite and chlorite will not form below 150°C. The fact that core temperatures are slightly colder than their suggested threshold temperature could indicate that water in the MH-2 core is cooling down. The two values are so close though that this difference could also be the result of measurement error, or of the cooling of well water during drilling and extraction, or of some other drilling-related process. The fact that alteration occurs in this zone where measured temperatures are so close to those proposed by Schmidt and Robinson is further support for their model.

### *Conclusions*

This investigation of the MH-2 Core had two major goals: to characterize the composition of what was an unknown basaltic core in an effort to determine geothermal feasibility, and to contribute to an ongoing debate regarding the transition from smectite to corrensite to chlorite. The project then had both a practical and intrinsic value as a contribution to a geothermal project and scientific question respectively.

We have found evidence for the dominance of smectite throughout the core, but also a zone with more complicated mineralogy. This zone, where fluid/rock ratios are high, appears to have corrensite and chlorite as well as smectite. If our data is in line with the model proposed by Shau and Pecor (1992), which it appears to be, then the altered zone is likely in equilibrium with the water and more mineralization is not occurring.

Much work remains to be done to clarify and confirm our findings. XRD, while useful for initial characterization, has several limitations. Because samples are crushed and analyzed only for minerals present, we could be missing entirely processes whereby different minerals are altered to different clays. The three clay minerals could be growing in separate parts of the same sample but this distinction does not appear with XRD. Petrographic analysis will help describe textures of the core and could show where and how clay alterations are occurring. Microprobe analysis should be performed to determine mineral compositions. This will help us to characterize the interlayers better and will provide further evidence for or against randomly interstratified C-S. Future work should also include fluid flow and composition analysis to investigate the particulars of the hydrothermal alteration. Fracture pattern analysis will help in overall characterization the core, and will indicate where hydrothermal alterations are possible.

### **Acknowledgements**

This work was sponsored by DOE award DE-EE0002848, and by the International Continental Drilling Program (GFZ-Potsdam, Germany). Additional support for continued drilling at Mountain Home AFB was provided by the US Air Force Air Combat Command. Vassar College XRD facilities were supported by NSF grant EAR-1229257. We would also like to thank Nathan Henderson from Bruker Analytical for his continued help with the XRD instrument and software, and John Shervais from Utah State University/Project Hotspot for his help with the core. I, Joe

Wheeler, would also like to thank my advisor (and co-author) Jeff Walker. Without his endless enthusiasm and support none of this would have been possible.

## **References Cited**

- Aly, M. H., Rodgers, D. W., Thackray, G. D., & Hughes, S. S. (2009). Recent magmatotectonic activity in the Eastern Snake River Plain-Island Park region revealed by SAR interferometry. *Journal of Volcanology and Geothermal Research*, 188(1-3), 297-304.
- Beaufort, D. & Meunier, A. (1994). Saponite, corrensite, and chlorite-saponite mixed layers in the Sancerre-Couy deep drill-hole (France) *Clay Minerals*, 29, 47-61.
- Bettison-Varga, L., & Mackinnon, I. D. R. (1997). The role of randomly mixed-layered chlorite/smectite in the transformation of smectite to chlorite. *Clays and Clay Minerals*, 45(4), 506-516.
- Breckenridge, R. P., Nielson, D. L., Shervais, J. W., & Wood, T. R. (2012). Exploration and resource assessment at Mountain Home Air Force Base, Idaho, using an integrated team approach. Paper presented at the *Transactions - Geothermal Resources Council*, , 36 1 615-619.
- Dekayir, A., Amouric, M., & Olives, J. (2005). Clay minerals in hydrothermally altered basalts from Middle Atlas, Morocco. *Clay Minerals*, 40(1), 67-77.
- Moore, D. M., & Reynolds, R. C. (1997). *X-ray diffraction and the identification and analysis of clay minerals* (1st ed.). Oxford: Oxford University Press.

- Murakami, T., Sato, T., & Inoue, A. (1999). HRTEM evidence for the process and mechanism of saponite-to-chlorite conversion through corrensite. *American Mineralogist*, 84(7-8), 1080-1087.
- Nelson, S. (2011, November 29). Phyllosilicates. *Tulane University*. Retrieved May 6, 2013, from <http://www.tulane.edu/~sanelson/eens211/phyllsilicates.htm>
- Roberson, H. E., Reynolds Jr., R. C., & Jenkins, D. M. (1999). Hydrothermal synthesis of corrensite: A study of the transformation of saponite to corrensite. *Clays and Clay Minerals*, 47(2), 212-218.
- Robinson, D., & Santana De Zamora, A. (1999). The smectite to chlorite transition in the Chipilapa Geothermal System, El Salvador. *American Mineralogist*, 84(4), 607-619.
- Schiffman, P., & Fridleifsson, G.O. (1991) The smectite-chlorite transition in drillhole NJ-15, Nesjavellir geothermal field, Iceland: XRD, BSE and electron microprobe investigations. *Metamorphic Geology*, 9, 679-696
- Schmidt, S. T., & Robinson, D. (1997). Metamorphic grade and porosity and permeability controls on mafic phyllosilicate distributions in a regional zeolite to greenschist facies transition of the North Shore Volcanic Group, Minnesota. *Geological Society of America Bulletin*, 109(6), 683-697.
- Shau, Y. -, & Peacor, D. R. (1992). Phyllosilicates in hydrothermally altered basalts from DSDP hole 504B, leg 83 - a TEM and AEM study. *Contributions to Mineralogy and Petrology*, 112(1), 119-133.

Shervais, J. W., Evans, J. P., Christiansen, E. J., Schmitt, D. R., Liberty, L. M., Blackwell, D. D., Glen, J.M., Kessler, J.E., Potter, K.E., Jean, M.M., Sant, C.J., Freeman, T. G. (2011). Hotspot: The Snake River Geothermal Drilling Project - an overview. Paper presented at the *Transactions - Geothermal Resources Council*, 35 2 995-1003.